THE JOURNAL OF COMPARATIVE NEUROLOGY 455:100–112 (2003)

Two Ribbon Synaptic Units in Rod Photoreceptors of Macaque, Human, and Cat

KAREN MIGDALE,[1] STEVE HERR,[1] KARL KLUG,[2] KAREEM AHMAD,[1] KEN LINBERG,[3] PETER STERLING,[4] AND STAN SCHEIN[1,2]*

[1]Department of Psychology, University of California, Los Angeles, Los Angeles, California 90095-1563

[2]Brain Research Institute, University of California, Los Angeles, Los Angeles, California 90095-1761

[3]Neuroscience Research Institute, University of California, Santa Barbara, Santa Barbara, California 93106

[4]Department of Neuroscience, University of Pennsylvania, Philadelphia, Pennsylvania 19104

ABSTRACT

The rod photoreceptor's synaptic terminal (or *spherule*) uses an elaborate synaptic structure to signal absorption of one or more photons to its postsynaptic targets. This structure includes one *or* two synaptic ribbons inside the terminal and a pouch-like "invagination" outside the terminal, into which enter a widely variable number of incoming fibers and postsynaptic targets—central elements supplied by rod bipolar cells and lateral elements supplied by horizontal cells. Nonetheless, our three-dimensional reconstructions of this synaptic structure in foveal retina of macaque monkey and peripheral retina of human and cat reveal several features that are highly conserved across species and with eccentricity: 1) every spherule has one invagination; 2) with rare exceptions, every spherule has two *ribbon synaptic units* with these features: a) on the presynaptic side, each ribbon synaptic unit has a ribbon or part of a ribbon and one trough-shaped arciform density that demarcates its active zone; b) on the postsynaptic side, each ribbon synaptic unit has two apposed lateral elements and one or more central elements; 3) the volume of the extracellular space in the single invagination is small, ~0.1 μm^3; and 4) the largest distance from active zone to receptor regions on bipolar cells is small, less than ~1.5 μm. With such small dimensions, release of one quantum of transmitter can pulse glutamate to a concentration comparable to the EC_{50} of the metabotropic glutamate receptors on the central elements associated with both synaptic units. We speculate that two ribbon synaptic units are required to sustain the high quantal release rate needed to signal a single photon. J. Comp. Neurol. 455: 100–112, 2003.

Indexing terms: presynaptic terminals; synapses; retina; synaptic membranes; rods (retina); endocytosis

After Hecht, Shlaer, and Pirenne (1942) showed that human rod photoreceptors could respond to absorption of a single photon, investigators sought an explanation at the level of the rod outer segment. They were rewarded by the discovery of a small but measurable reduction of inward current in amphibian rods (Baylor et al., 1979) and later in monkey rods (Baylor et al., 1984) in response to absorption of a single photon. Attention eventually turned to the structure and function of the synaptic terminal of the rod, called the *spherule*, because its synapse must be able to transmit the small hyperpolarization (Schneeweis and Schnapf, 1995) resulting from absorption of a single photon (Falk and Fatt, 1974; Rao et al., 1994). One challenge to any such analysis of the rod synapse is the great variation in structure from rod spherule to rod spherule in a given retina (Missotten, 1965; Grünert and Martin, 1991; Rao-Mirotznik et al., 1995). Moreover, one might

Grant sponsor: National Institute of Health; Grant numbers: R01 EY11153, R01 EY06096, R01 EY08124, and RO1 EY00888; Grant sponsor: IMH; Grant number: MH15795-18; Grant sponsor: the University of California, Los Angeles Academic Senate.

*Correspondence to: Stan Schein, Department of Psychology, Franz Hall, Mailcode 951563, University of California, Los Angeles, CA 90095-1563. E-mail: schein@ucla.edu

Received 29 January 2002; Revised 6 August 2002; 13 September 2002

DOI 10.1002/cne.10501

Published online the week of November 11, 2002 in Wiley InterScience (www.interscience.wiley.com).

expect the spherule's dimensions to vary with eccentricity, as is the case with cone terminals (Chun et al., 1996). In this paper we report on human, monkey, and cat rod spherules, focusing on what does vary and, more importantly, what does not.

The rod spherule (Fig. 1A) is 2–3 μm in diameter, but postsynaptic elements invaginate it to form a pouch that is roughly 1 μm across. In some regions of some sections these elements appear to form a *triad*, comprised of two lateral elements (LE) and one central element (CE) (Fig. 1C) (Sjöstrand, 1958; Missotten, 1962, 1965). However, the invaginating elements more generally form complex configurations (e.g., Fig. 1D) that require reconstruction to identify elements and spatial organization. Horizontal cells provide the lateral elements (Missotten, 1965; Stell, 1965, 1967), and rod bipolar cells provide the central elements (Sjöstrand, 1958; Missotten, 1965). The most prominent presynaptic structure associated with the triad is the flat, synaptic ribbon (Sjöstrand, 1953; Ladman, 1958; McCartney and Dickson, 1985), which appears as a stripe in cross section (e.g., Fig. 1C). The synaptic ribbon is bedecked with a reservoir of synaptic vesicles on both sides. The arciform density (Ladman, 1958), at the base of the synaptic ribbon, appears as an arc in cross section but is shaped like a trough in three dimensions (Fig. 1C). The active zone, where calcium channels are located and where synaptic vesicles fuse with the presynaptic membrane and release their quanta of transmitter, flanks the arciform density (Raviola and Gilula, 1975; Morgans, 2001).

Missotten (1965) found considerable variation in morphology from his examination of the spherules of 50 human rods and reconstruction of many of them. The features that varied included the number of ribbons (generally one or two), the number of fibers supplying central elements (from one to five), and the number of fibers supplying lateral elements (from two to three). Grünert and Martin (1991) reported similar variations in a study of 28 monkey rods. Moreover, macaque rods immunocytochemically stained for bassoon, a marker of synaptic ribbons, show one or two ribbons, or occasionally three (cf. Fig. 1D of Haverkamp et al., 2001).

Even the standard cross-sectional view of a triad admits multiple three-dimensional interpretations. Rao-Mirotznik et al. (1995) found, as a rule, two lateral elements and two central elements in cat rod spherules and coined the term *tetrad* to describe their findings. They also reported finding a

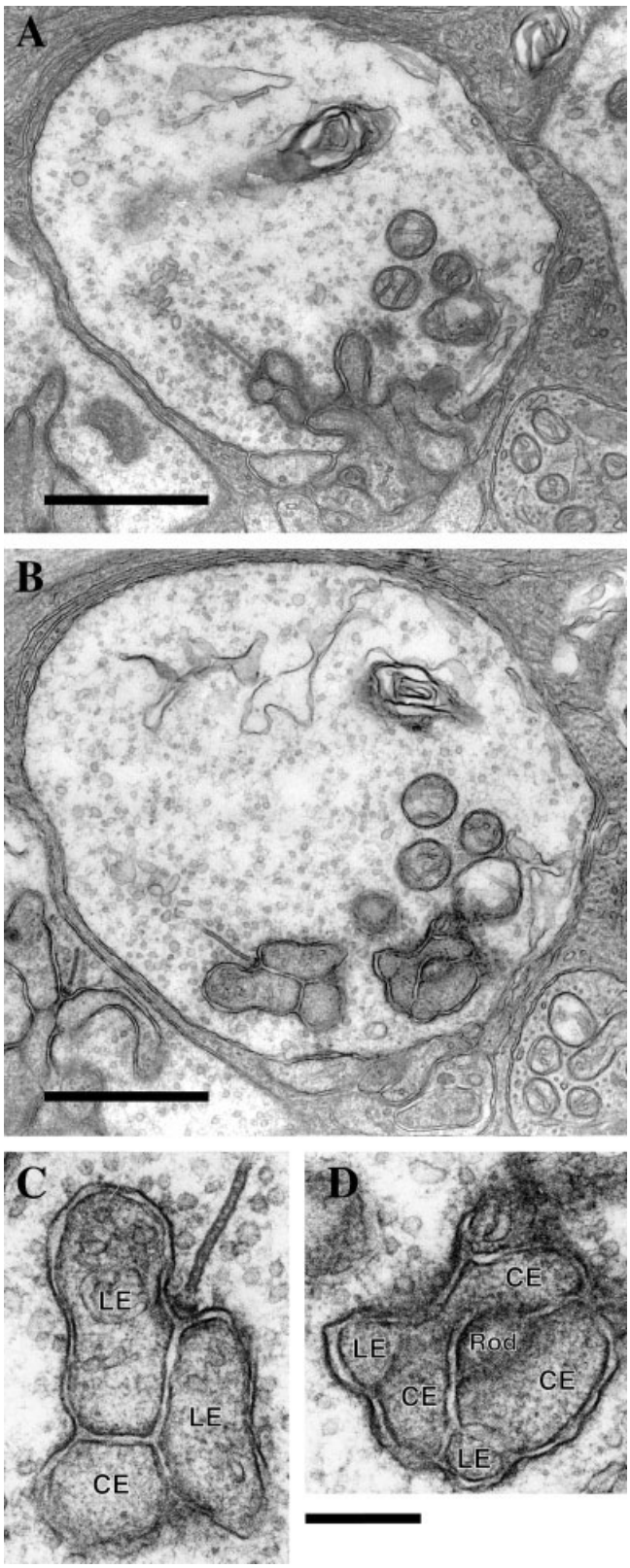

Fig. 1. Electron micrographs of cross sections of monkey rod spherule #m53. **A:** The outer surface of monkey rod spherule #m53 folds inside itself at the bottom, creating an opening, through which bipolar and horizontal cell fibers enter, and a pouch (or "invagination") that is filled by the invaginating fibers and the central and lateral elements at their distal ends. **B:** The left side of this section—four sections from the one shown in A—shows a standard "triad" of three postsynaptic elements, shown enlarged in C. The right side shows a more complex configuration, enlarged in D. **C:** Enlargement of the triad on the left in Figure 1B. The presynaptic side has a synaptic ribbon, an arciform density at the base of the ribbon, a narrow cleft between the (horizontal cell) lateral elements (LE), a (bipolar) central element (CE), and a bifurcation of the cleft over the central element. **D:** Enlargement of the tangle of elements on the right in Figure 1B. Labels are as in C; in addition, "Rod" refers to the interior of the rod spherule, where it forms a "finger." Scale bars = 1 μm in A,B; 0.25 μm in D (applies to C,D).

single ribbon with one long active zone marked by one long arciform density. They suggested that the horseshoe shape of the ribbon improved proximity of the quantal release sites alongside the arciform density to the postsynaptic elements. Indeed, their diffusion calculations suggested that a single quantum of glutamate triggers a postsynaptic potential in *all* of the postsynaptic elements within the invagination of the spherule.

We reconstructed a rod spherule in our foveal series of sections initially because of the novelty of looking at rods in the fovea, where their incidence is low. Surprised by its three-dimensional features, we went on to reconstruct rod spherules over a wide range of eccentricity and of several species of animal. In the face of substantial variation that one would have expected, we identified several unvarying features: Each of these disparate spherules had a single invagination. Each invagination contained nearly the same, small volume of extracellular space. The distances from quantal release sites to target elements were correspondingly small. Of particular importance, we showed that the main organizing feature in spherules is the *ribbon synaptic unit*, containing all or part of one ribbon, one arciform density, one active zone, a pair of apposed lateral elements, and one or more central elements. With rare exceptions, each spherule had exactly two of these ribbon synaptic units. We speculate that each ribbon synaptic unit is associated with machinery that can perform endocytosis at some maximal rate (e.g., 50 coated pits sec^{-1}) and that two synaptic units are needed to sustain the high, continuous rate of exoctyosis (e.g., 100 quanta sec^{-1}) required to signal absorption of a single photon (Rao-Mirotznik et al., 1998; van Rossum and Smith, 1998).

MATERIALS AND METHODS

We examined serial electron micrographs of 90-nm thin sections of nine macaque rod spherules (Fig. 1). Because of lateral displacement of photoreceptor terminals from inner segments (Schein, 1988), the center of the region corresponded to ~1° of eccentricity in the visual field (Calkins et al., 1994). Rods are absent in the foveola, but the fovea in Macaque has a radius of 500 μm, or 2.5°, so the photoreceptors that contacted this region were well within the fovea (Polyak, 1941). The methods for preparation of this material have been described in detail previously (Tsukamoto et al., 1992; Calkins et al., 1994).

In brief, after perfusion fixation (glutaraldehyde plus paraformaldehyde) of a 6-kg, male *Macaca fascicularis* monkey, a retina was postfixed with 2% OsO_4, stained en bloc with 1% uranyl acetate, dehydrated, and embedded in Epon, and the foveal region described was serially sectioned. The sections were mounted, poststained with uranyl acetate and lead citrate, and photographed in an electron microscope. We also examined serial electron micrographs of 20 peripheral, human rod spherules that were used previously in a study by Linberg and Fisher (1988). This human retinal tissue was thick-sectioned and then serially thin-sectioned (80 nm) radially. The sections were stained with uranyl acetate and lead citrate. The methods for preparation of this material are described in detail in Linberg and Fisher (1986). Finally, we examined serial electron micrographs of three cat rods that were used previously in a study by Rao-Mirotznik et al. (1995).

All of the 32 rods were examined in detail. Two monkey rods, four human rods, and three cat rods were also digitally reconstructed with Montage software (Smith, 1987), tiled with Contour Fitter (Meyers et al., 1992), rotated and viewed in stereo with Geomview (University of Minnesota Geometry Center—http://www.geom.umn.edu/software/geomview/), and rendered with the Blue Moon Rendering Tools (http://www.bmrt.org).

Ribbon lengths were measured along the bottom edge of the ribbon (the edge facing the presynaptic membrane) after the ribbon was reconstructed. Arciform density lengths were measured from the same reconstructions. The volume of extracellular space (ECS) in the spherule's invagination was also measured from reconstructions as follows: The Contour Fitter software provided the surface areas of all the membranes within the invagination, specifically that of the spherule itself, the invaginating horizontal cell fibers, and the invaginating bipolar cell fibers. Because the clefts that comprise the ECS are bounded by two membranes, ECS volume was calculated as the product of cleft width (10 nm) (Ribble et al., 1997) and half of the total membrane surface area. The distances from individual arciform density points to individual bifurcation points were the lengths of straight lines connecting them.

RESULTS

The cross section in Figure 1A through a rod spherule from monkey shows how the outer surface membrane invaginates to form a small pouch into which postsynaptic elements enter. Figure 2A shows a reconstruction of just the *outer surface* of the spherule, along with its one synaptic ribbon. Figure 2B adds the spherule membrane that constitutes the *invagination*. Like all spherules, this spherule has one invagination and thus a single "opening" through which postsynaptic elements enter, shown as a hole in Figure 2A, and by the slightly occluded dark outline in Figure 2B. If we add the invaginating horizontal cell and bipolar cell elements (Fig. 2C), one can see that the spherule membrane of the invagination closely overlies the invaginating elements. The volume contained within this spherule is 4.5 μm^3. The volume contained within the invagination is 0.62 μm^3, 14% as much. Assuming a spherical geometry, these volumes correspond to diameters of 2.05 μm and 1.06 μm.

Three-dimensional structure

The cross section in Figure 1C shows the standard triplet of postsynaptic elements that define a triad, namely, two lateral elements and a central element. It also shows, on the presynaptic side, a synaptic ribbon and the arciform density at the base of the ribbon. These features, which are color-coded in Figure 3A for use in the reconstructions that will be shown later, include white and blue for back and front lateral elements, orange stripes for the ribbon, yellow circles for the arciform density, and variously colored central elements. After quantal release, the path of glutamate diffusion runs down the cleft between the two apposed lateral elements and bifurcates over the tops of the central element (Fig. 1C). We have marked this *bifurcation point* in Figure 3A with an orange circle.

The three-dimensional structures associated with this triad are shown in Figure 3B. At the top of this figure, within the spherule, the surface of the synaptic ribbon appears nearly planar. (Subsequent figures will show that the ribbon surface generally curves.) The arciform density, an arc-shaped structure that runs along most of the base

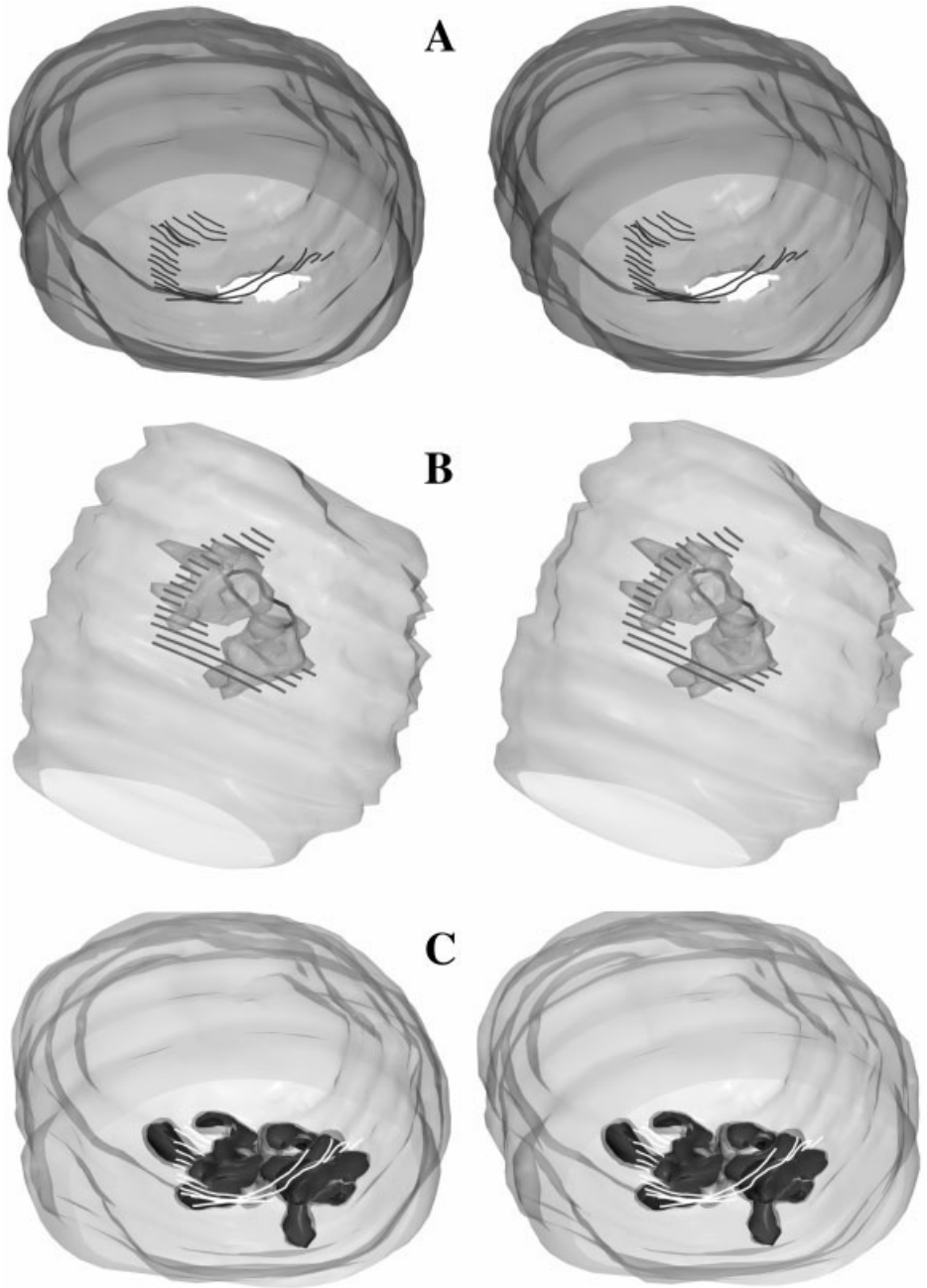

Fig. 2. Stereo reconstruction of monkey rod spherule #m53 from serial, vertical sections like the one shown in Figure 1A. To see the three-dimensional surfaces in this and subsequent figures, readers should cross their eyes. **A:** This side view of the (transparent) outer surface of the whole spherule leaves out the invaginated part of the spherule membrane. A window in the side of the spherule makes it easier to see the synaptic ribbon, shown by the black lines, and the rim of the invagination, the "opening" in the floor of the spherule. **B:** This top view of the spherule includes the synaptic ribbon and the invaginated spherule membrane. **C:** This side view is the same view as in A. Along with showing the (black) invaginating horizontal cell and bipolar cell elements, it illustrates how closely the (partially transparent) spherule membrane overlies the invaginating elements.

of the ribbon, forms a trough that cradles the edge of the ribbon closest to the cell membrane, but it is represented here as a series of yellow spheres, one from each section. These *presynaptic* structures are enclosed by the spherule membrane, so they are in the interior of the spherule.

The spherule membrane, which creates the invagination, appears in Figure 3B as a white drape over the back lateral element and a blue drape over the front lateral element. (The lateral elements themselves are not shown here.) Bipolar cell elements are shown in blue, red, yellow, and green. Along the tops of the bipolar (central) elements, the string of orange bifurcation points forms a ridgeline. The bifurcation ridgeline and its associated central elements, as well as the lateral elements, are *outside* the

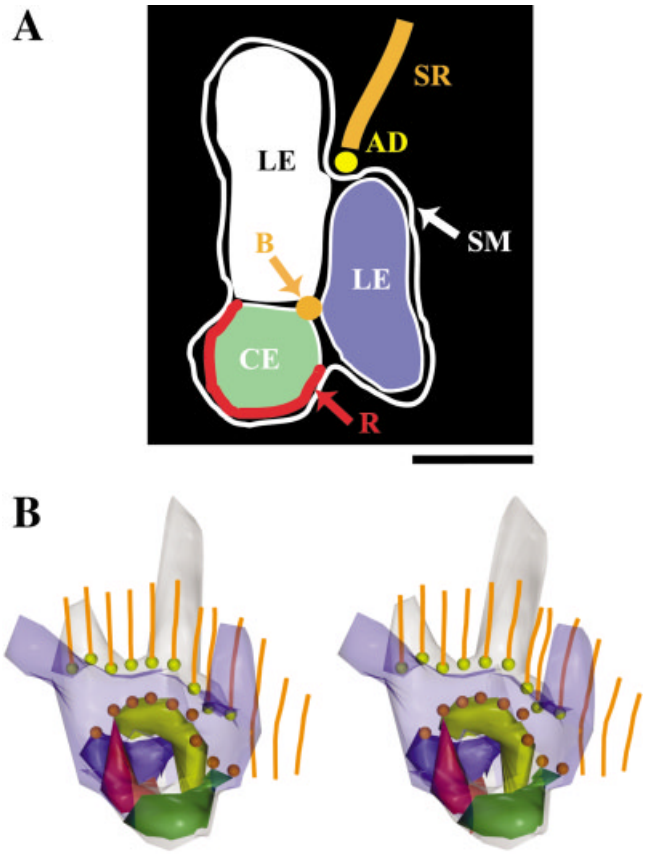

Fig. 3. Two-dimensional (A) and three-dimensional (B) structure of a ribbon synaptic unit. **A:** Color coding of Figure 1C, for use in the reconstructions of Figures 3B and 4–7. A standard triad has three postsynaptic elements, two apposed lateral elements (LE), and one central element (CE). In this figure and Figures 4–7, back lateral elements are colored *white* and front lateral elements are colored *blue*. The central element, shown here in green, may be various colors in subsequent figures. The orange stripe is the synaptic ribbon (SR). The yellow circle at the base of the ribbon marks the arc-shaped arciform density (AD). The orange circle marks the bifurcation point (B), where the diffusion path of glutamate bifurcates over the central element. Metabotropic glutamate receptors (R) cluster in the region of the central element that is in contact with rod spherule membrane (SM). **B:** Three-dimensional structure of the ribbon synaptic unit associated with the triad shown in A. Starting at the top of the figure, the synaptic ribbon is nearly planar in three dimensions. The arciform density, shaped like a trough, is represented by a series of yellow spheres. The spherule membrane, which creates the invagination, appears as a white drape over the back lateral element and a blue drape over the front lateral element. The lateral elements themselves are not shown. The transparent spherule membrane also overlies bipolar-cell central elements colored blue, red, yellow, and green. Along the tops of the central elements, the string of orange bifurcation markers forms a ridgeline. Additional images of this structure but without the spherule membrane can be seen at the upper left in Figures 4B and C. Scale bar = 0.25 μm in A.

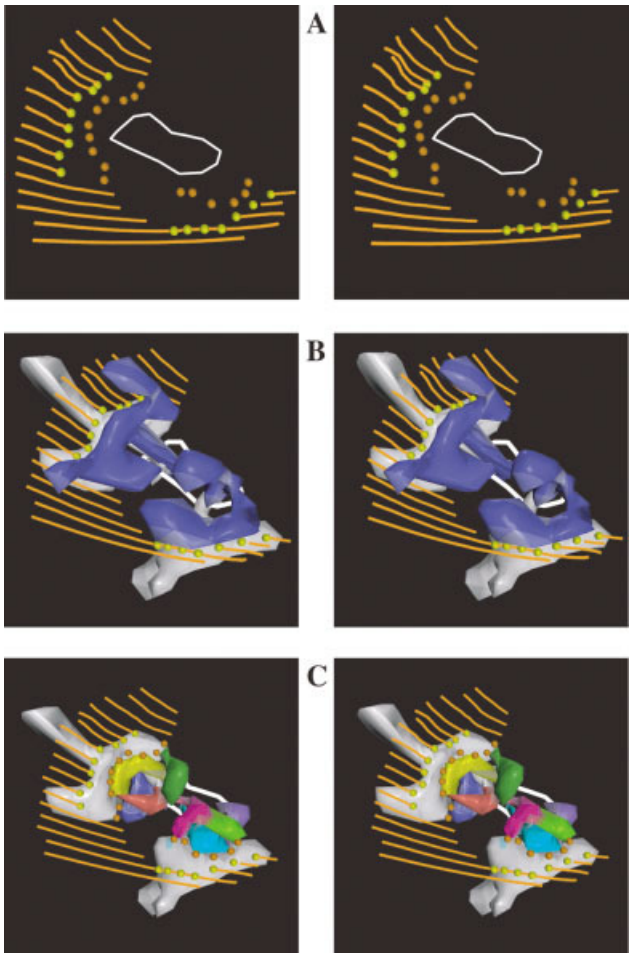

Fig. 4. Stereo reconstruction of monkey rod spherule (#m53) with one ribbon, a gap between two arciform densities, and four lateral elements. Color coding follows Figure 3A. **A:** The ribbon is continuous, but the arciform density structure at its base is in two parts, separated by a gap, giving two arciform densities. The length along the base of this ribbon is 3.3 μm, and the lengths of its arciform densities are 0.8 μm and 0.9 μm. Also shown here are the two strings of bifurcation markers that comprise two bifurcation ridgelines. The single "opening" on the floor of the spherule indicates that there is a single invagination. **B:** The ribbon, its arciform densities, and two pairs of apposed lateral elements, which are provided by four horizontal cell fibers that enter the single opening in the floor of the spherule. Each pair of lateral elements is associated with an arciform density. Postsynaptic (lateral) elements are absent in the "gap" region between the arciform densities. **C:** The ribbon, the two back lateral elements, the two arciform densities, the two bifurcation ridgelines over the central elements, variously colored central elements in single file underneath each of the two bifurcation ridgelines, and the opening on the floor of the spherule. Four central elements are associated with the first ribbon synaptic unit. Three central elements and an additional bipolar cell process that fails to reach the arciform density are associated with the second ribbon synaptic unit. Four bipolar cell fibers enter through the single opening to supply the eight bipolar cell elements within the invagination.

spherule membrane but *inside* the pouch-like invagination.

The full variation in structure that we have observed in the nine digitally reconstructed monkey, human, and cat rod spherules is illustrated in Figure 4 (monkey fovea, spherule containing one ribbon), Figure 5 (monkey fovea, two ribbons), Figure 6 (human periphery, two ribbons), and Figure 7 (cat, one ribbon). In each of these figures, part A shows the ribbon(s) and arciform densities, part B adds the invaginating horizontal cell (lateral) elements, and part C subtracts the occluding, front lateral element and adds the invaginating bipolar (central) elements.

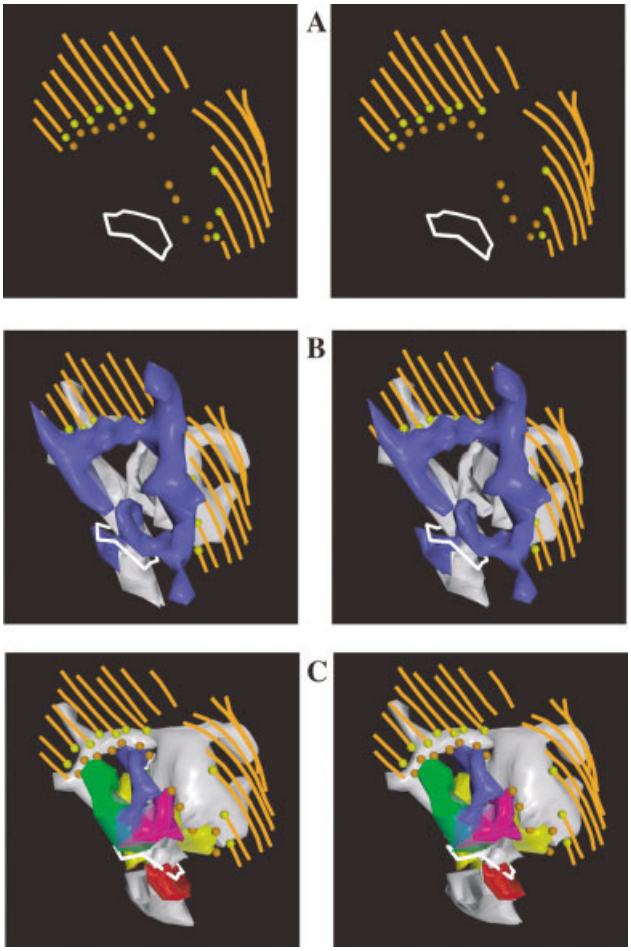

Fig. 5. Stereo reconstruction of a rod spherule (#m31) from monkey with two ribbons and four lateral elements. Color coding follows Figure 3A. **A:** Each of the two ribbons has its own arciform density and a bifurcation ridgeline. The ribbons are 1.3 μm and 1.6 μm long, and their arciform densities are 0.8 μm and 0.6 μm long. Also shown here is the single opening in the floor of the spherule. **B:** Two ribbons, the arciform densities, and the four lateral elements, which are provided by two horizontal cell fibers that enter the single opening. The white horizontal cell fiber divides to give rise to both white lateral elements. The blue horizontal cell fiber forms two blue lobes, each apposed to one of the white lateral elements. **C:** The ribbon, the two back lateral elements, the two arciform densities, two bifurcation ridgelines, variously colored central elements, and two (non-central) bipolar cell elements that do not reach as high as the bifurcation ridgeline. Each ribbon synaptic unit is associated with two central elements in single file and one non-central element. Three bipolar cell fibers enter through the opening in the floor of the spherule to supply the five bipolar cell elements within the invagination.

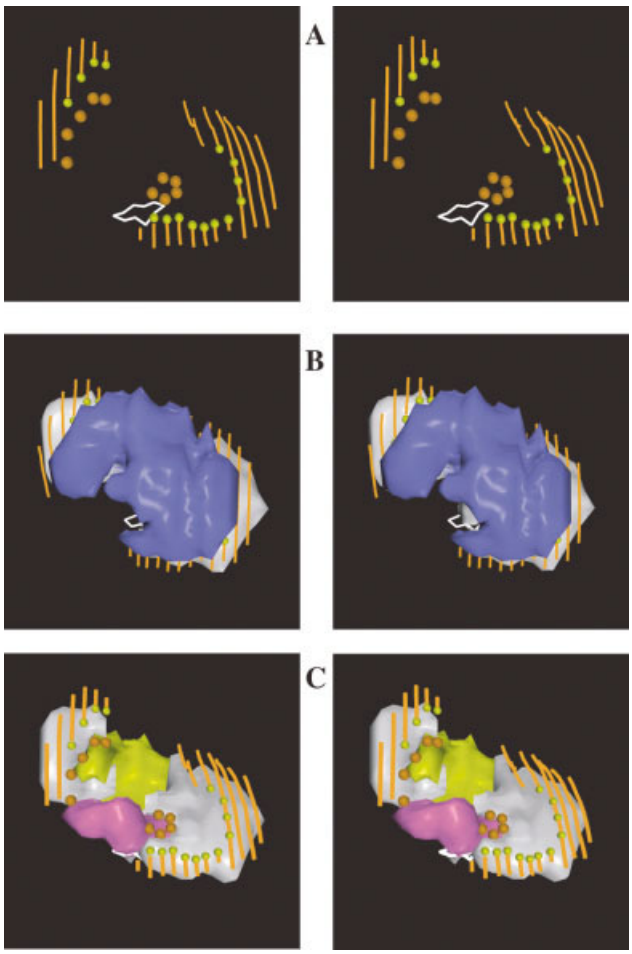

Fig. 6. Stereo reconstruction of human rod #h18 with two ribbons and three lateral elements. Color coding follows Figure 3A. **A:** Each of the two ribbons has an arciform density and a bifurcation ridgeline. The ribbons are 1.8 μm and 1.0 μm long, and their arciform densities are 1.1 μm and 0.5 μm long. Also shown here is the single opening. **B:** Two ribbons, the arciform densities, and the three lateral elements that are provided by just one horizontal cell fiber that enters the opening. The large, middle lateral element does double duty, enabling the three lateral elements to form two apposed pairs of lateral elements. To serve in this manner, the middle lateral element is comprised of two lobes. **C:** Two ribbons, the two back lateral elements, the two arciform densities, two bifurcation ridgelines, and two central elements in single file associated with one bifurcation ridgeline and one central element associated with the other. Two bipolar cell fibers enter the opening to supply the two central elements within the invagination.

These elements fill the invagination, as was shown in Figures 1 and 2, and are coated by the spherule membrane. For this reason, the spherule membrane in Figures 4–7 is implied but not shown.

Ribbons and arciform densities

Nearly all our rod spherules, 31 of 32, have one or two ribbons (Table 1). (One monkey spherule has three.) In general, spherules with one ribbon have two arciform densities separated by a gap (Figs. 4A, 7A). The exceptions in the cat are discussed below.) Spherules with two ribbons (Figs. 5A, 6A) have one arciform density at the base of each ribbon, so those spherules also have a total of two arciform densities. Twenty-nine of the 32 spherules have two arciform densities (Table 1). (One of the exceptions is the monkey spherule with three ribbons and three arciform densities, so 30 of the 32 have at least two arciform densities.)

In primate spherules with one ribbon we find an interruption (or "gap") in the arciform density, as can be seen in Figure 4A. Two other features accompany this gap. In this region, the spherule has no postsynaptic elements (Fig.

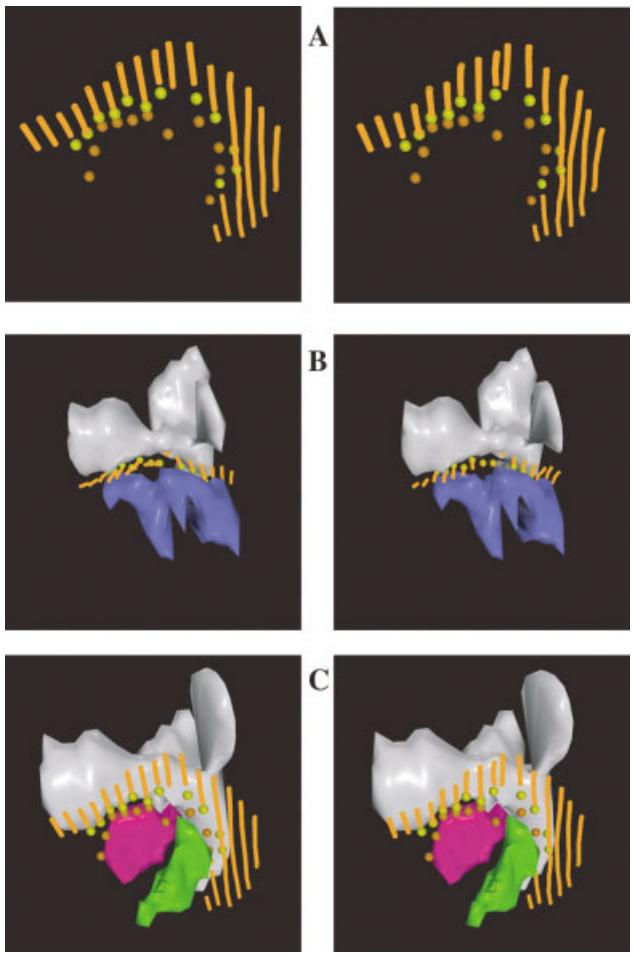

Fig. 7. Stereo reconstruction of cat rod #c7 with one ribbon, a small gap between two arciform densities, and two lateral elements. Color coding follows Figure 3A. **A:** The ribbon is continuous, but the arciform density structure at its base is in two parts, separated by a small gap. Correspondingly, there are two bifurcation ridgelines. The length along the base of this ribbon is 2.4 μm, and the lengths of its arciform densities are 0.6 μm and 0.6 μm. **B:** The ribbon, its two arciform densities, and the two lateral elements that are provided by two horizontal cell fibers. Both lateral elements are comprised of two lobes, giving four lobes in total, organized into two apposed pairs. **C:** The ribbon, the single back lateral element with two lobes, the two arciform densities, two bifurcation ridgelines, and two central elements. Two bipolar cell fibers supply the two central elements.

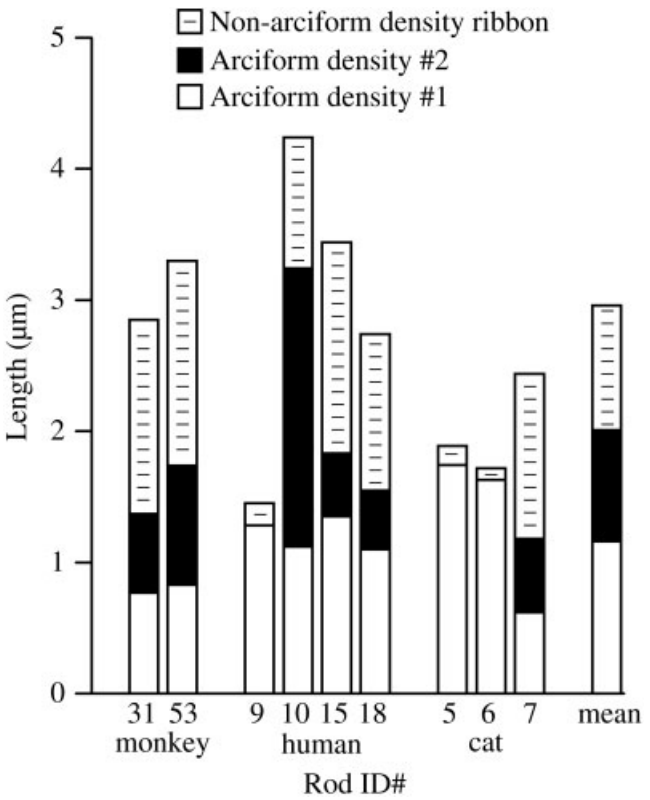

Fig. 8. Lengths of arciform densities and remaining (non-arciform density) ribbon. Some of these spherules, specifically monkey #53 and cat #7, have one ribbon with two arciform densities. Some (monkey #31, human #10, human #15, and human #18) have two ribbons, with one arciform density per ribbon. Others (cat #5, cat #6, and the anomalous human #9) have one ribbon with one arciform density. "Non-arciform density ribbon" (lined bars) refers to the part of the bottom edge of the ribbon that is not cradled by an arciform density.

4C), and the ribbon is not up against the spherule membrane (Fig. 2B). Indeed, we looked for and initially discovered the gap in the arciform density *after* we had noticed these other two features.

The total length of ribbon varies considerably, as does the length of an individual arciform density (Fig. 8). By contrast, if one excludes human spherule #h10, the total length of the (one or two) arciform densities per spherule is more constant.

Openings

Figures 4–6 also show the opening at the base of the invagination, through which horizontal and bipolar cell fibers invaginate the rod spherule. Every spherule that we examined has a single opening (Table 1) and thus a single invagination.

Lateral elements

Thirty-one of 32 rod spherules have *two pairs* of apposed lateral elements. (One has three.) The wide variety of arrangements that provide these two pairs of lateral elements is illustrated in parts B of Figures 4–7: four lateral elements derived from four horizontal cell fibers (Fig. 4B), four lateral elements derived from two horizontal cell fibers that branch to form separate lobes (Figs. 5B, 7B), and three lateral elements supplied by one horizontal cell fiber (Fig. 6B). (We apply the term "fiber" to bipolar dendrites and horizontal cell terminals as they enter the opening, before they branch inside the invagination to end as "elements.") Many rod spherules are like the one in Figure 6B in having *three* lateral elements that are configured as *two apposed pairs*, with the blue element serving both pairs; in some cases, the single lateral element is sandwiched between the other two lateral elements.

In 29 of 29 primate rod spherules, each of the two postsynaptic pairs of apposed lateral elements is associated with one of the presynaptic arciform densities (Figs. 4–6). This is also the case for the cat spherule (#c7) shown

TABLE 1. Numbers of Structures Related to Ribbon Synaptic Units in Rod Spherules

ID#	Invag.[1]	Ribbons	Gaps	Arciform densities	Bifur.[1] ridges	Ribbon synaptic units
A. Macaque monkey						
m31	1	2	0	2	2	2
m53	1	1	1	2	2	2
m201	1	1	1	2	2	2
m202	1	3	0	3	3	3
m203	1	1	1	2	2	2
m204	1	1	1	2	2	2
m205	1	1	1	2	2	2
m206	1	2	0	2	2	2
m207	1	1	1	2	2	2
B. Human						
h1	1	2	0	2	2	2
h2	1	2	0	2	2	2
h3	1	2	0	2	2	2
h4	1	1	1	2	2	2
h5	1	2	0	2	2	2
h6	1	2	0	2	2	2
h7	1	2	0	2	2	2
h8	1	2	0	2	2	2
h9	1	1	1	2	2	2
h10	1	2	0	2	2	2
h11	1	2	0	2	2	2
h12	1	2	0	2	2	2
h13	1	2	0	2	2	2
h14	1	2	0	2	2	2
h15	1	2	0	2	2	2
h16	1	2	0	2	2	2
h17	1	2	0	2	2	2
h18	1	2	0	2	2	2
h19	1	2	0	2	2	2
h20	1	2	0	2	2	2
C. Cat						
c5	1	1	0[2]	1	2	2
c6	1	1	0[2]	1	2	2
c7	1	1	1[3]	2	2	2

[1]Invag., invaginations; Bifur; bifurcation.
[2]Although there is no gap, the ribbon twists where the two pairs of lateral elements abut.
[3]The arciform density has a very small gap, just one section long.

in Figure 7, although the gap between the two arciform densities associated with the single ribbon in that spherule is just one section and could easily be missed. Note that the ribbon twists at the point of the gap, and the part of the ribbon surface associated with one arciform density is in a different geometric plane from the part of the ribbon surface associated with the other arciform density. (The twist in the synaptic ribbon can also be seen in primate spherules with one ribbon, e.g., Fig. 4.) The other two cat spherules, with two pairs of apposed lateral elements and a twist in the ribbon at the point where these two pairs abut, are just like #c7, except that there is no gap in their single arciform density at the twist.

Central elements

To visualize the central elements in context, they were added to the figures, and the front (blue) lateral elements were removed so as not to obscure them. Therefore, parts C in Figures 4–7 shows the ribbon or ribbons, their arciform densities, the back lateral elements in white, and variously colored central elements lined up in single file underneath each arciform density. In Figure 4C, four central elements line up under one arciform density, and another three line up under the other. At the other end of the spectrum (e.g., Fig. 7C), just one central element might be associated with each of the two arciform densities.

We placed bifurcation markers (orange spheres) at the points where the synaptic cleft bifurcates over a central element to form a ridge in three dimensions (cf. Fig. 3). Regardless of their number, central elements line up in single file under and between a pair of apposed lateral elements (parts C in Figs. 4–7). As a result, the bifurcation markers, at the top of the central elements, also line up under and between each pair of apposed lateral elements to form a single ridgeline. Thirty-two of 32 rods have two bifurcation ridgelines (Table 1), each associated with a pair of apposed lateral elements.

Some bipolar cell dendrites fail to reach the bifurcation ridgeline. Such "non-central" elements are illustrated by the purple one in Figure 4C and the red and one of the yellow ones in Figure 5C.

In primate rods, each bifurcation ridgeline is associated with a single arciform density (as illustrated in parts A of Figs. 4–6), and, as mentioned above, each arciform density is associated with a pair of apposed lateral elements. These statements apply to the cat rod spherule shown in Figure 7 as well, but not to the other two cat spherules in our study, each of which has no gap and just one arciform density. However, each cat spherule has a twist in its ribbon—where the two pairs of apposed lateral elements abut—and two bifurcation ridgelines. Similarly, McCartney and Dickson (1985; their Fig. 2) show guinea pig rods with one ribbon, and that ribbon has a twist like the ones in the cat spherules. Thus, in these latter cases, the break between the two bifurcation ridgelines corresponds to a twist in the ribbon but without a gap to divide the arciform density structure into two troughs.

Output streams

The features that are constant among our rod spherules—one opening, two arciform densities, two pairs of apposed lateral elements, and two bifurcation ridgelines—coexist with wide variation in other features. For example, the number of ribbons is generally one or two, although there is one case with three (Table 1). The number of horizontal cell *fibers* ranges from one to four (Fig. 9A), and the number of *lateral elements* that emerge from those fibers ranges from two to four (Fig. 9B), arranged in a variety of configurations, as shown in parts B of Figures 4–7. The number of bipolar cell *fibers* ranges from two to four (Fig. 9A), and the number of *central elements* ranges from two to seven (Fig. 9B). As noted above, an occasional bipolar cell process fails to reach a central position between the apposed pair of lateral elements (e.g., Figs. 4C, 5C), and the number of such *non-central* (bipolar) elements ranges from zero to two (Fig. 9B).

One interpretation of our findings is that each rod has *two* output streams, with the glutamate flowing from one active zone (flanking one arciform density) to its associated central elements, and the glutamate from the other active zone going to its associated central elements. An alternative interpretation is that each rod has *one* output stream, with every central element having access to the quanta of glutamate released at either active zone. To investigate these ideas, we measured the volume of extracellular space (ECS) into which one quantum of glutamate might diffuse and the maximum distances between release and receptor sites.

Even though the rods in our study came from different animals and from widely varying eccentricities, and even though the surface areas of horizontal cell, bipolar cell, and rod spherule membranes varied considerably from one rod to the next, total surface area ($20.3 \pm 2.7\ \mu m^2$) varied remarkably little (Fig. 10A). We measured cleft

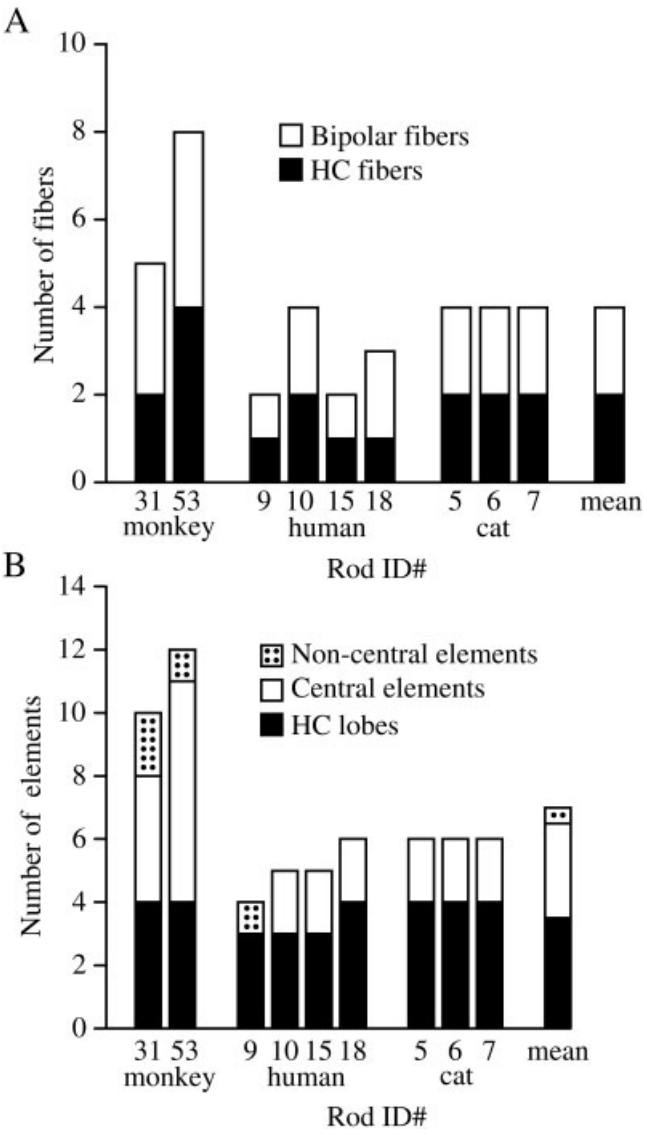

Fig. 9. Numbers of horizontal and bipolar cell fibers and elements. **A:** Fibers, horizontal cell (HC), and bipolar cell, are defined at the opening into the invagination. **B:** Elements, lateral, central, and non-central bipolar cell, are counted within the invagination at their distal ends.

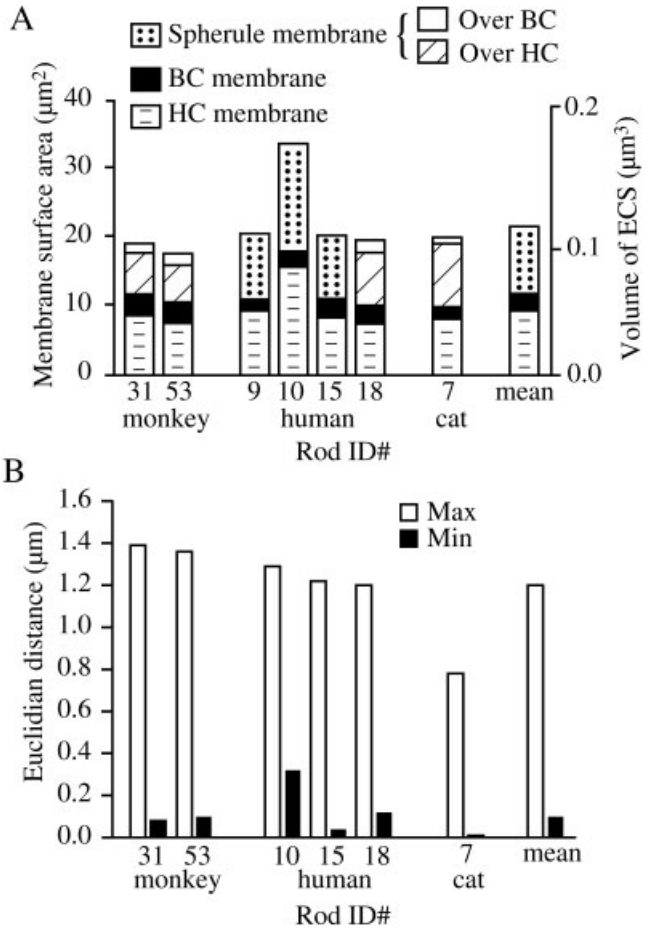

Fig. 10. Dimensions within the spherule. **A:** The surface area of membrane within the invagination is the sum of the surface areas of bipolar cell (BC) membrane, horizontal cell (HC) membrane, and rod spherule membrane. All spherule membrane in the invagination is apposed to bipolar and horizontal cell elements; these are represented separately for monkey spherules #31 and #53, human spherule #18, and cat spherule #7 by open and hatched bars. The volume of extracellular space (ECS) is computed here as the product of half of the total membrane surface area and the (10-nm) width of the space between membranes. **B:** The maximum and minimum euclidean distances from an arciform density point to a bifurcation point within each spherule.

width as 10 nm (Ribble et al., 1997). Because clefts are everywhere bounded by two membrane surfaces, to compute ECS we divided these total surface areas by two before multiplying by that width (Fig. 10A). Although cleft width is difficult to measure accurately, and our value could be subject to debate, the low degree of variation holds for ECS as well, irrespective of what value we used for cleft width.

We estimated maximum distances by two methods. First, from measurements of the total volume contained within the invagination, we computed the diameter of a sphere of that volume and found a range from 1.1 μm to 1.5 μm. Second, because the invagination is not exactly a sphere, we measured the maximum distances between each arciform density and the bifurcation ridge associated with the other arciform density. In practice, this meant measuring the distances between the arciform density markers of one arciform density to all of the bifurcation markers associated with the other arciform density, which we did for two monkey, three human, and one cat spherules. These maxima range from 1.1 μm to 1.4 μm (Fig. 10B).

The maximum distance from the arciform density of one active zone to the bifurcation ridgeline of the other, however, imperfectly reflects the maximum distance from glutamate release sites to glutamate receptor sites. First, vesicles fuse with presynaptic membrane in the active zones flanking the arciform density (Raviola and Gilula, 1975). In Figure 1C that distance is slightly less than 0.1 μm. Second, the (mGluR6) metabotropic glutamate receptors on the central elements appear to be located in the

TABLE 2. Bipolar Elements

Spherule	Central elements	Non-central elements	Apposition regions	Apposition area (μm^2)
Monkey #53	7	1	12	1.9 μm^2
Monkey #31	4	2	18	1.4 μm^2
Human #18	2	0	2	2.2 μm^2
Cat #7	2	0	2	1.1 μm^2

Central and non-central bipolar elements and the numbers and areas of their regions of apposition with rod spherule membrane. Numbers of central and non-central elements are also shown in Figure 9B. These four rod spherules are the ones shown in Figures 4–7.

regions where those central elements are contacted by spherule membrane (Fig. 4A of Vardi et al., 2000), similar to the situation for cone bipolar cells where they are contacted by cone pedicle membrane (Vardi et al., 2000). These contact regions, marked as R in Figure 3A, are approximately 0.2 μm from the bifurcation marker, beyond the bifurcation ridgeline and the contacts between central elements and lateral elements.

Receptor areas

Vardi et al. (2000) note that ". . . rod and cone membranes that face the mGluR6 receptor always display a 'fluffy' density. This density is so distinctive that it could be used as a marker for the location of the mGluR6 receptor in ON bipolar cell dendrites that are not immunostained." Examination of serial sections shows that virtually 100% of the regions of contact between the spherule and central elements in our monkey material exhibit such densities. Each central element can have two receptor regions, one on each side of the central element, or they may coalesce into one, as in Figure 3A. In fact, the four central elements associated with the *left* arciform density in Figure 4C have among them seven separate regions in contact with spherule membrane. The seven central elements and one non-central bipolar-cell process associated with *both* arciform densities in this spherule have a total of 18 contact regions (Table 2). Similarly, the rod in Figure 5 has 12 contact regions. By contrast, the rod spherules in Figures 6 and 7 have just two contact regions, one for each central element. Nonetheless, the areas of contact in the rods in Figures 4–7 are fairly similar, 1.9 μm^2, 1.4 μm^2, 2.2 μm^2, and 1.1 μm^2, respectively (Table 2).

DISCUSSION

Triads and ribbon synaptic units

The term *triad*, as originally defined by Missotten (1965), denoted a group of *three postsynaptic elements*, two lateral elements and one central element, associated on the presynaptic side with a synaptic ribbon. Missotten himself was more impressed with triads in cones: "Each cavity contains three terminal buds; as a rule they join up into a triad, so that each terminal bud touches the pedicle and is in contact with the two others" (Missotten, 1965, p. 76). With regard to the rod, he was more circumspect: "In some synapses one of [the small terminal buds] is inserted between two big terminal buds, so that a picture is formed which resembles the triad found in the pedicle of the cones. However, this arrangement is often asymmetric and the triad not conspicuous" (Missotten, 1965, p. 57). As an illustration of the difficulty, Figure 1B shows, in addition to the classic *triad* on the left, a complicated configuration on the right, the latter enlarged in Figure 1D. Reconstruction (Fig. 4) and resectioning by computer in a different plane are required to show that the configuration on the right is actually a second triad.

In the context of the historical and current use of the term triad to refer to three postsynaptic elements, we believe that our three-dimensional perspective clarifies the synaptic arrangement within the rod spherule and requires introduction of a new term, the rod *ribbon synaptic unit*. The rod ribbon synaptic unit is comprised of the following: on the presynaptic side, a ribbon or part of a ribbon and its coextensive arciform density and associated active zone; on the postsynaptic side, two apposed lateral elements and one or more central elements lined up in single file at the level of the bifurcation ridgeline (Fig. 3). As shown here, a single rod ribbon may support one or more ribbon synaptic units.

As suggested by Missotten, the synaptic arrangements in mammalian cones are simpler to interpret than those seen in the rod; nonetheless, just as we have shown in the rod spherule, a synaptic ribbon in a cone may be presynaptic to more than one pair of apposed lateral elements, and each pair of lateral elements may embrace more than one central element (Chun et al., 1996; Herr et al., 2003). Therefore, this notion of a ribbon synaptic unit applies not only to the ribbon synaptic arrangements in rod spherules but also to the ribbon synaptic arrangements in cone pedicles.

Chun et al. (1996) has proposed redefining the term *triad*: "Instead of inventing new terms such as 'tetrades' or 'pentades' we use the name triad to describe an invaginating synaptic complex, which comprises a presynaptic ribbon and two lateral horizontal cell elements." We agree with the intent behind this redefinition of the word *triad*, which focuses on a pair of apposed lateral elements to define a "unit" of ribbon synaptic anatomy. However, we respectfully disagree with counting to three by adding one *presynaptic* ribbon to two *postsynaptic* lateral elements, which runs counter to historical use of the term *triad*. Nonetheless, we understand why Chun et al. (1996) chose not to include central elements in the count, because there may be one, giving a *triad*, or more than one, giving a *tetrad* (Rao-Mirotznik et al., 1995), a *pentad*, etc.

Two ribbon synaptic units in each rod spherule

The major finding of this paper is that mammalian rod spherules, with rare exceptions, have two ribbon synaptic units, as just defined, even though some spherules have one synaptic ribbon and some have two. This simplification emerges in spite of wide variations in structure, number of ribbons, numbers of horizontal and bipolar cell fibers that enter the invagination, and numbers of lateral and central elements into which those fibers branch. This finding applies to human and monkey rods, in which we and others have found as many as a dozen elements within the invagination, as well as to a sample of cat rods, in which we and one of our collaborators (Rao et al., 1994) found a *tetrad* of elements, two central and two lateral.

This description of the mammalian rod spherule is new. Missotten's 1965 summary diagram of a rod spherule, reproduced here as Figure 11A, shows just one ribbon

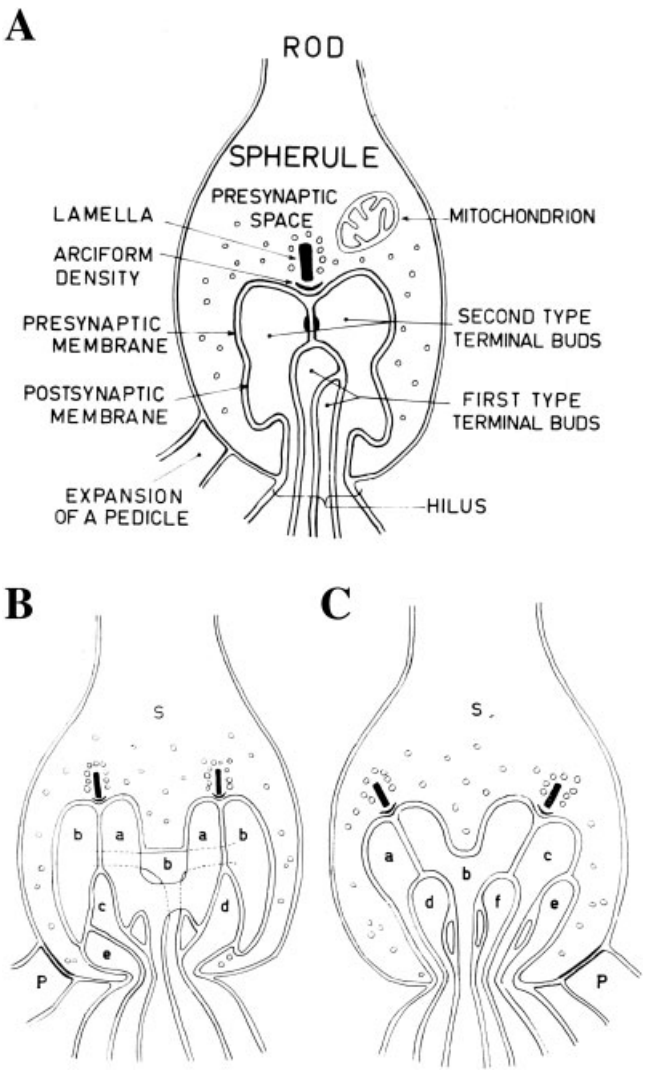

Fig. 11. Diagrams of the invagination in rod spherules from Figures 15 (**A**), 23 (**B**), and 26 (**C**) of Missotten (1965). **A:** We interpret this summary diagram to mean that a rod spherule has one ribbon synaptic unit, with one pair of apposed lateral elements and two central elements, not necessarily in single file underneath the arciform density. The labels translate to currently used terms as follows: "lamella" to synaptic ribbon, "first type of terminal bud" to central element, "second type of terminal bud" to lateral element, and "hilus" to opening. **B,C:** These diagrams schematize the three-dimensional reconstruction of the invaginations in two human rod spherules. In retrospect, one can see that each invagination has two ribbon synaptic units, each with a synaptic ribbon, an arciform density, a pair of apposed lateral elements, and multiple central elements.

synaptic unit with two lateral elements and two central elements (one of which will take the central position in another section). This misleading picture has held sway since then. Ironically, Missotten's diagrams of the structure of two reconstructed rod spherules (Figs. 11B,C) from the same monograph correctly show two ribbon synaptic units, each with its own synaptic ribbon, pair of lateral elements (or lobes), and central elements.

Constancy in the face of variation among rod spherules

The reproducible presence of two ribbon synaptic units clarifies the anatomy of the mammalian rod spherule and supersedes the wide variation in numbers of lateral elements, central elements, and ribbons. Our findings also establish constancy in the face of variation in several other features. On the presynaptic side, the total length of active zone, as measured by the length of arciform density, is fairly constant among rod spherules across species and with eccentricity.

On the postsynaptic side, the metabotropic mGluR6 receptors appear to be located in the region of the bipolar cell central elements that are apposed to rod spherule membrane, although the evidence is stronger for central elements apposed to cone pedicle membrane (Vardi et al., 2000). (Due to diffusion of reaction product in that study, however, localization of mGluR6 receptors in cone as well as rod bipolar cells is not as precise as would be desirable.) Even though the number of such regions varies widely, from 2 to 18 in our material, the total surface area of these regions, from 1.1 to 2.2 μm^2, varies remarkably little across species and with eccentricity.

The volume of ECS in the invagination and the maximum distance from the arciform density to receptor patches in the rod spherule also vary little. In retrospect, such a low degree of variation should not be surprising, because the spatiotemporal concentration profile of glutamate in the synaptic clefts of the rod spherule depends critically on these dimensions (Rao-Mirotznik et al., 1998).

Why two rod ribbon synaptic units?

Each ribbon synaptic unit has its own pair of apposed lateral elements, so insofar as negative feedback from horizontal cells utilizes a local mechanism (Kamermans et al., 2001), glutamate release at each active zone would appear to be under independent control by its lateral elements. This notion would be even more interesting if each ribbon synaptic unit comprised a separate signaling stream, that is, if the glutamate released at one active zone diffused to the glutamate receptors on the central elements of that synaptic unit but not to the glutamate receptors on the central elements of the other. Figure 4C, for example, shows separate aggregates of bipolar central elements under each bifurcation ridge.

However, receptor patches are not up against the bifurcation ridge. As a result, many of the receptor patches of the central elements of one ribbon synaptic unit are as close to the active zone of the other ribbon synaptic unit as they are to their own. Our measurements show that the receptor regions associated with the active zone of one ribbon synaptic unit are generally much closer than 1.5 μm to the active zone of the other ribbon synaptic unit, and diffusion can transport glutamate over these distances in $\sim$1 msec or less. Also, both ribbon synaptic units are contained within just one invagination, as evidenced by the presence of a single opening, and the volume of the extracellular space is small. As a result, one synaptic vesicle's worth of glutamate produces a concentration pulse within the entire extracellular space (Rao-Mirotznik et al., 1998) that is

comparable to the EC_{50} (10 μM) of the mGluR6 receptors in cat rod bipolar cells (de la Villa et al., 1995).

This last conclusion would not be weakened by the presence of glutamate transporters in the synaptic cleft. In particular, the intervals between continuous quantal release events, believed to be on the order of ~10 msec, are much shorter than the transport time of glutamate transporters, on the order of tens of milliseconds (Danbolt, 2001). Moreover, physiological data suggest that transporters on Müller cells carry out initial clearance of glutamate, with transporters on the membranes of rods and rod bipolar cells—presumably also outside the invagination—primarily involved in retrieving glutamate subsequently released by Müller cells (Pow et al., 2000).

With a single signaling stream, if the maximum release rate were 50 quanta sec^{-1} from each active zone (Lagnado et al., 1996), two active zones would enable central elements to experience 100 quanta sec^{-1}, the minimum rate suggested by the analyses of Rao-Mirotznik et al. (1998) and van Rossum and Smith (1998) to signal a single photon. However, there is reason to doubt that 50 quanta sec^{-1} is a limit to the rate of exocytosis. For example, in the giant bipolar terminal in goldfish, each ribbon synapse can release as many as 100 quanta in 0.2 seconds, a rate of 500 quanta sec^{-1} (von Gersdorff et al., 1996).

However, the latter release conditions in the bipolar terminal exhaust the pool of ~100 synaptic vesicles associated with each ribbon (von Gersdorff et al., 1996), so this rate cannot be sustained, and release of additional quanta must wait for replenishment mechanisms, such as endocytosis. Coincidentally, with a time constant for endocytosis of ~2 seconds (von Gersdorff and Matthews, 1994; Neves and Lagnado, 1999), recharging the ~100 synaptic vesicles associated with each ribbon would proceed at a maximal rate of ~50 sec^{-1} (Lagnado et al., 1996; von Gersdorff et al., 1996). We therefore speculate that the *maximal rate of endocytosis* by the machinery associated with an active zone may set the upper limit for the *sustainable* rate of continuous *exocytosis* from that active zone, and the presence of two (or even three) ribbon synaptic units doubles (or even triples) the sustainable quantal release rate.

ACKNOWLEDGMENTS

We thank Dr. Yoshihiko Tsukamoto, Patricia Masarachia, and Sally Shrom for preparing the EM material, and Kazuki Uema and Lisa Travis for printing. We also thank Robert Smith for helpful discussions. Portions of this work were presented earlier in abstract form (Migdale et al., 1998).

LITERATURE CITED

Baylor DA, Lamb TD, Yau, K-W. 1979. Responses of retinal rods to single photons. J Physiol (Lond) 288:613–634.

Baylor DA, Nunn BJ, Schnapf JL. 1984. The photocurrent, noise, and spectral sensitivity of rods of the monkey *Macaca fascicularis*. J Physiol (Lond) 357:575–607.

Calkins DJ, Schein SJ, Tsukamoto Y, Sterling P. 1994. M and L cones in macaque fovea connect to midget ganglion cells by different numbers of excitatory synapses. Nature 1994 371:70–72.

Chun M-H, Grünert U, Martin PR, Wässle H. 1996. The synaptic complex of cones in the fovea and in the periphery of the macaque monkey retina. Vis Res 36:3383–3395.

Danbolt NC. 2001. Glutamate uptake. Prog Neurobiol 65:1–105.

de la Villa P, Kurahashi T, Kaneko A. 1995. L-glutamate-induced responses and cGMP-activated channels in three subtypes of retinal bipolar cells dissociated from the cat. J Neurosci 15:3571–3582.

Falk G, Fatt P. 1974. The dynamic voltage-transfer function for rod-bipolar cell transmission. Vis Res 14:739–741.

Grünert U, Martin PR. 1991. Rod bipolar cells in the macaque monkey retina: immunoreactivity and connectivity. J Neurosci 11:2742–2758.

Haverkamp S, Grünert U, Wässle H. 2001. The synaptic architecture of AMPA receptors at the cone pedicle of the primate retina. J Neurosci 21:2488–2500.

Hecht S, Shlaer S, Pirenne MH. 1942. Energy, quanta, and vision. J Gen Physiol 25:819–840.

Herr S, Klug K, Sterling P, Schein S. 2003. Inner S-cone bipolar cells provide all of the central elements for S cones in macaque retina. J Comp Neurol. In press.

Kamermans M, Fahrenfort I, Schultz K, Janssen-Bienhold U, Sjoerdsma T, Weiler R. 2001. Hemichannel-mediated inhibition in the outer retina. Science 292:1178–1180.

Ladman AJ. 1958. The fine structure of the rod-bipolar cell synapse in the retina of the albino rat. J Biophy Biochem Cytol 4:459–466.

Lagnado L, Gomis A, Job C. 1996. Continuous vesicle cycling in the synaptic terminal of retinal bipolar cells. Neuron 17:957–967.

Linberg KA, Fisher SK. 1986. An ultrastructural study of interplexiform cell synapses in the human retina. J Comp Neurol 243:561–576.

Linberg KA, Fisher SK. 1988. Ultrastructural evidence that horizontal cell axon terminals are presynaptic in the human retina. J Comp Neurol 268:281–297.

McCartney MD, Dickson DH. 1985. Photoreceptor synaptic ribbons: three-dimensional shape, orientation and diurnal (non)variation. Exp Eye Res 41:313–321.

Meyers D, Skinner S, Sloan K. 1992. Surfaces from contours. ACM Trans Graph 11:228–258.

Migdale K, Herr S, Klug K, Linberg K, Sterling P, Schein S. 1998. Triads in primate rods and cones. Invest Ophthalmol Vis Sci Suppl 39:S412.

Missotten L. 1962. L'ultrastructure des cônes de la rétine humaine. Bull Soc Belge Ophtalmol 130:472–502.

Missotten L. 1965. The ultrastructure of the retina. Brussels: Editions Arscia SA.

Morgans CW. 2001. Localization of the alpha(1F) calcium channel subunit in the rat retina. Invest Ophthalmol Vis Sci. 42:2414–2418.

Neves G, Lagnado L. 1999. The kinetics of exocytosis and endocytosis in the synaptic terminal of goldfish retinal bipolar cells. J Physiol 515: 181–202.

Polyak SL. 1941. The retina. Chicago: University of Chicago Press.

Pow DV, Barnett NL, Penfold P. 2000. Are neuronal transporters relevant in retinal glutamate homeostasis? Neurochem Int 37:191–198.

Rao R, Buchsbaum G, Sterling P. 1994. Rate of quantal transmitter release at the mammalian rod synapse. Biophys J 67:57–63.

Rao-Mirotznik R, Harkins AB, Buchsbaum G, Sterling P. 1995. Mammalian rod terminal: architecture of a binary synapse. Neuron 14, 561–569.

Rao-Mirotznik R, Buchsbaum G, Sterling P. 1998. Transmitter concentration at a three-dimensional synapse. J Neurophysiol 80:3163–3172.

Raviola E, Gilula NB. 1975. Intramembrane organization of specialized contacts in the outer plexiform layer of the retina. J Cell Biol 65:192–222.

Ribble J, Klug K, Sterling P, Schein SJ. 1997. The cleft system associated with a foveal cone terminal in Macaque. Invest Ophthalmol Vis Sci 38:S723.

Schein SJ. 1988. Anatomy of macaque fovea and spatial densities of neurons in foveal representation. J Comp Neurol 269:479–505.

Schneeweis DM, Schnapf JL. 1995. Photovoltage in rods and cones in the macaque retina. Science 268:1053–1056.

Sjöstrand FS. 1953. The ultrastructure of the inner segments of the retinal rods of the guinea pig eye as revealed by electron microscopy. J Cell Comp Physiol. 42:45–70.

Sjöstrand FS. 1958. Ultrastructure of retinal rods synapses of the guinea pig eye as revealed by three-dimensional reconstructions from serial sections. J Ultrastruct Res 2:122–170.

Smith RG. 1987. Montage: a system for three-dimensional reconstruction by personal computer. J Neurosci Methods 21:55–69.

Stell WK. 1965. Correlation of retinal cytoarchitecture and ultrastructure in Golgi preparations. Anat Rec 153:389–397.

Stell WK. 1967. The structure and relationship of horizontal cells and photoreceptor bipolar synaptic complexes in goldfish retina. Am J Anat 121:401–424.

Tsukamoto Y, Masarachia P, Schein SJ, Sterling P. 1992. Gap junctions between the pedicles of macaque foveal cones. Vis Res 32:1809–1815.

Vardi N, Duvoisin R, Wu G, Sterling P. 2000. Localization of mGluR6 to dendrites of ON bipolar cells in primate retina. J Comp Neurol 423: 402–412.

van Rossum MC, Smith RG. 1998. Noise removal at the rod synapse of mammalian retina. Vis Neurosci 15:809–821.

von Gersdorff H, Matthews G. 1994. Dynamics of synaptic vesicle fusion and membrane retrieval in synaptic terminals. Nature 367:735–739.

von Gersdorff H, Vardi E, Matthews G, Sterling P. 1996. Evidence that vesicles on the synaptic ribbon of retinal bipolar neurons can be rapidly released. Neuron 16:1221–1227.